CAMBRIDGE
UNIVERSITY PRESS

Article

Crystal chemistry and origin of REE-bearing mukhinite from carbonate veins of the Svetlinsky gold deposit, South Urals, Russia

Victor G. Korinevsky[1,#], Nikita V. Chukanov[2,3], Sergey M. Aksenov[4,5*] , Evgeniy V. Korinevsky[1], Vasiliy A. Kotlyarov[1], Dmitry A. Zamyatin[6], Anastasiya D. Ryanskaya[6], Sergey V. Kolisnichenko[1], Svetlana M. Lebedeva[1] and Vera N. Ermolaeva[7]

[1]South Urals Federal Research Center of Mineralogy and Geoecology of the Uralian Branch of the Russian Academy of Sciences, Miass, Chelyabinsk oblast 456317, Russia; [2]Institute of Problems of Chemical Physics, Russian Academy of Sciences, Chernogolovka, Moscow region, 142432, Russia; [3]Faculty of Geology, Moscow State University, Vorobievy Gory, Moscow, 119991, Russia; [4]Laboratory of Nature-Inspired Technologies and Environmental Safety of the Arctic, Kola Science Centre, Russian Academy of Sciences, Apatity 184209, Russia; [5]Geological Institute, Kola Science Centre, Russian Academy of Sciences, 14 Fersman Street, Apatity 184209, Russia; [6]Institute of Geology and Geochemistry of the Uralian Branch of the Russian Academy of Sciences, Ekaterinburg 620016, Russia and [7]Institute of Experimental Mineralogy, Russian Academy of Sciences, Chernogolovka, Moscow region, 142432, Russia

Abstract

A rare earth element (REE)-, Cr- and Mg-bearing variety of the vanadium epidote-group mineral mukhinite occurs in a calcite–dolomite carbonatite dyke cutting metamorphosed volcano-sedimentary rocks exposed in the walls of the quarry of the Svetlinsky gold deposit, South Urals. This mineral was found in a paragene assemblage including native sulphur, phlogopite and fluorophlogopite, together with accessory pyrite, other sulfides and sulfosalts, gold, Cr- and V-bearing muscovite, margarite, Cr- and V-bearing dravite, fluoro-tremolite, actinolite, fluoro-pargasite, anhydrite, apatite, uranium hydroxides, V-rich titanite, V- and Nb-rich rutile, spinel and corundum. The contents of ΣREE_2O_3 and V_2O_3 in mukhinite vary in the ranges of 4.01–9.69 and 5.34–7.46 wt.%, respectively. A Raman spectrum of REE-rich mukhinite is provided. The main schemes of isomorphic substitutions in mukhinite are $\Sigma REE + Mg \leftrightarrow Ca + Al$ and $V+Cr \leftrightarrow Al$. The crystal structure of REE-rich mukhinite has been studied by single-crystal X-ray diffraction analysis. The mineral is monoclinic, with the space group $P2_1/m$, and unit-cell parameters are: $a = 8.8972(11)$ Å, $b = 5.6221(6)$ Å, $c = 10.1519(12)$ Å, $\beta = 115.169°$ and $V = 459.60(11)$ Å^3. The crystal structure of REE-rich mukhinite is similar to that of its synthetic analogue; the refined crystal-chemical formula of the sample studied is $(Z = 2)$: $\{^{A1}Ca^{A2}(Ca_{0.8}REE_{0.2})\}\{^{M1}(Al_{0.95}Cr_{0.05})^{M2}Al^{M3}[(V,Cr)^{3+}_{0.40}Al_{0.35}Mg_{0.25}]\}(Si_2O_7)(SiO_4)O(OH)$.

Keywords: REE-rich mukhinite, epidote group, crystal structure, carbonatites, Svetlinsky gold deposit, South Urals

Introduction

Mukhinite $Ca_2(Al_2V^{3+})[Si_2O_7][SiO_4]O(OH)$ is a rare vanadium mineral of the epidote group (Shepel and Karpenko, 1965; Armbruster *et al.*, 2006). Until recently, it was known from only three locations in Russia which are situated in Western Siberia (Shepel and Karpenko, 1965; Konovalenko *et al.*, 2012), Kola Peninsula (Karpov *et al.*, 2013), South Urals (Tomilina *et al.*, 2016), and several localities in Slovakia (Uher *et al.*, 2008; Bačík and Uher, 2010; Bačík *et al.*, 2018). The geological setting of the three occurrences is rather different. Mukhinite from Kola Peninsula forms reaction rims around primary vanadium minerals (mainly coulsonite) in banded ores of the Pyrrhotite Gorge

deposit (Karpov *et al.*, 2013). At the Tashelginsky deposit, Western Siberia, mukhinite occurs in a skarn association together with diopside–hedenbergite, grossular, vesuvianite, hercynite, magnetite and corundum; the assemblage forms nests in marble (Shepel and Karpenko, 1965; Konovalenko *et al.*, 2012). In the third occurrence, near the village of Kvarkeno, Suunduk River basin, South Urals, mukhinite was found in a coarse-grained calcite marble in association with crystals of phlogopite, fluorite, pyrite, green muscovite and dravite (Tomilina *et al.*, 2016) (the authors associate the formation of mukhinite with the reaction of a hydrothermal fluid with the marble after the intrusion of granites of the Suunduk massif).

This paper describes a new find of mukhinite with an unusual REE-rich Mg- and Cr-bearing variety from a medium-grained calcite–dolomite dyke of a carbonate rock cutting metamorphosed volcano-sedimentary rocks exposed in the walls of the quarry of the Svetlinsky gold deposit, Plastovsky District, South Urals (Kolisnichenko and Popov, 2008). The crystal structure of natural mukhinite has been studied for the first time.

Geological setting and petrological data for calcite–dolomite dykes of the Svetlinsky deposit

Numerous thin (up to several tens of cm thick) meridional dykes of calcite–dolomite rocks are exposed in the eastern wall of the Svetlinsky quarry located on the East Uralian elevation at 26.7 km to the west of the town of Plast, Chelyabinsk region, Russia (54°17'45"N, 60°24'39"E). Brief descriptions can be found in Kolisnichenko and Popov (2008), Kolisnichenko *et al.* (2014), Korinevsky *et al.* (2019) and Korinevsky and Korinevsky (2020). These investigations provide geological and mineralogical evidence of the magmatic nature of these carbonate bodies rather than their metasomatic origin. The carbonate rocks form a set of closely spaced bodies (veins) dissecting the metamorphosed volcanic-terrigenous rocks.

Most carbonate rocks of the Svetlinsky deposit have a uniformly medium-grained massive texture. Lenticular (2.5–5 cm long) secretions of pale-yellow native sulphur and fluorophlogopite-enriched areas give the rocks a banded texture (Fig. 1a). The presence of sulfide impregnations and sulphur aggregates in the rocks causes a strong hydrosulfuric smell during crushing. When the carbonate rock powder is heated in an open flame, intense yellow–orange thermoluminescence is observed (Korinevsky *et al.*, 2019).

The carbonate veins of the Svetlinsky deposit are composed predominantly of a medium-grained calcite aggregate with subordinate dolomite grains (Fig. 2a, 3a), phlogopite, pyrite, quartz, and diverse accessory mineralisation which is confined mainly to quartz-rich bands.

In most cases, calcite is homogenous in composition. Usually, it contains magnesium (MgO ≈1 wt.%) and iron (FeO up to 3.25 wt.%). Occasionally, sulfur (up to 8.46 wt.% of SO_3) and uranium (up to 0.05 wt.% of UO_2) were detected as a result of the presence of submicroscopic inclusions of native sulphur (Korinevsky *et al.*, 2019) and uranium minerals. Some calcite grains contain syntactic growths of dolomite (Fig. 2a).

Accessory mineralisation, represented by small anhedral grains and euhedral crystals of various minerals, is distributed unevenly in carbonate rocks of the Svetlinsky deposit. The set of accessory minerals differs in different dykes. Usually, they are disseminated in the groundmass of the rock and are not confined to any cracks or veins. The most diverse accessories are observed in quartz-rich bands. Most individuals of accessory minerals have induction boundaries indicating their joint growth with carbonates and other minerals. No signs of metasomatic replacement of any minerals by other minerals have been found. The anhedral habit of sulfur and fluorite indicates that these minerals crystallised at the latest stages of the carbonate rocks formation.

Among accessory minerals, individuals of muscovite and fluorophlogopite, dravite, actinolite, tremolite, fluoro-tremolite, pargasite, ferrous spinel, corundum, margarite, fluorapatite, V- and Nb-bearing rutile, titanite, REE-rich mukhinite, uranium hydroxides, bastnäsite, vaesite, sulvanite, kalininite, patrónite, florensovite, gersdorffite, corundum (ruby), sphalerite, galena, gold and graphite have been identified. The total amount of accessory minerals in the carbonate rocks rarely exceeds 1–3 vol.%. Grains and crystals of some accessory minerals of the carbonate rocks are presented in Figs 3b–f and 4. Most of them contain essential amounts of V (Table 1).

A characteristic feature of some minerals associated with mukhinite (fluorophlogopite, dravite, muscovite, rutile and clinochlore) is the presence of significant amounts of vanadium (up to 2.5 wt.% of V_2O_3 in fluorophlogopite, 3.26 in dravite, 1.23 in
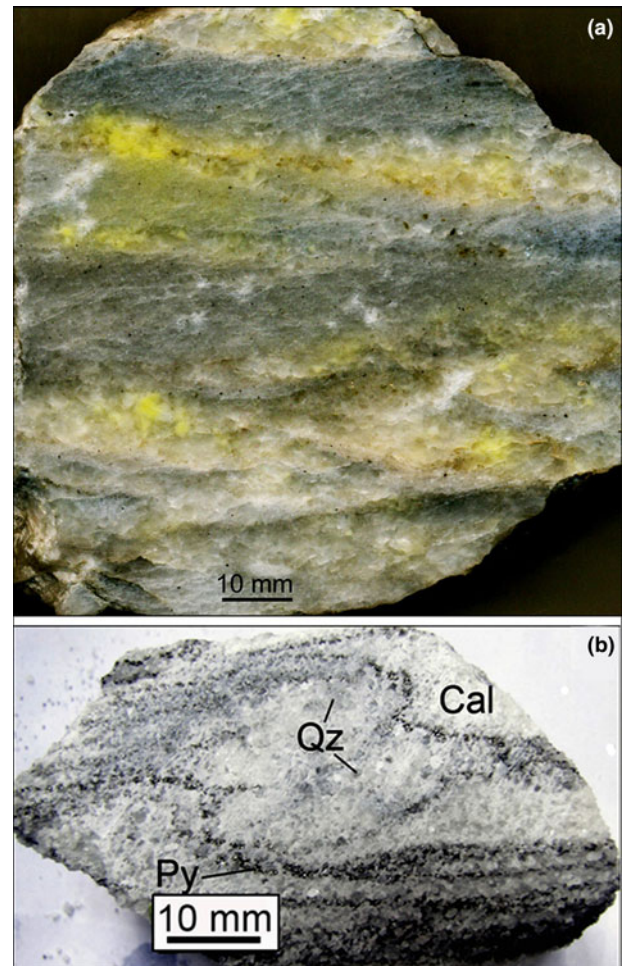

Fig. 1. (a) Banded texture of sulfur-containing phlogopitic calcite–dolomite rock in a fragment of the dyke from the Svetlinsky quarry; and (b) a specimen of essentially carbonate rock enriched in quartz (Qz) and fluorophlogopite with dark bands containing fine impregnation of pyrite (Py).

muscovite and 16.97 in rutile). Titanite (Fig. 5c) has unusually high contents of both V_2O_3 (up to 5.22 wt. %) and Al_2O_3 (up to 6.6 wt. %). In particular, the charge-balanced empirical formula of V-bearing titanite calculated on $(SiO_4)(O,OH)$ is $Ca_{1.00}(Ti_{0.61}Al_{0.30}V_{0.09})(SiO_4)[O_{0.61}(OH)_{0.39}]$. In muscovite, dravite, titanite and pargasite, chromium is also typically present, causing their bright green colour. Phlogopite is rich in fluorine; the F content reaches 5.92 wt.%, which corresponds to fluorophlogopite. Some grains of amphiboles are enriched in fluorine (up to 1.205 F atoms per formula unit (apfu) in fluoro-tremolite).

Within the grains of calcite, mukhinite and margarite, very small grains of a uranium mineral, probably representing uranium hydroxides are found repeatedly (Fig. 6). Small interstitial crystals of a uranium hydroxide with 87.69–91.02 wt.% UO_2 and 3.42–4.06 wt.% PbO (presumably, radiogenic lead) are observed occasionally between mukhinite and calcite individuals. Some grains have Th and La admixtures (ThO_2 up to 1.80 wt.% and La_2O_3 up to 1.48 wt.%). Around such crystals, zonal radiating rims of unusual REE-rich (with a predominance of La) minerals are occasionally observed (Fig. 6). Their compositions range as follows (wt.%): SiO_2 6.49–7.57, Al_2O_3 3.39–4.04, V_2O_3 1.30–1.50, MgO 0.24–0.51, CaO 9.03–9.46, La_2O_3 27.93–28.27, Ce_2O_3
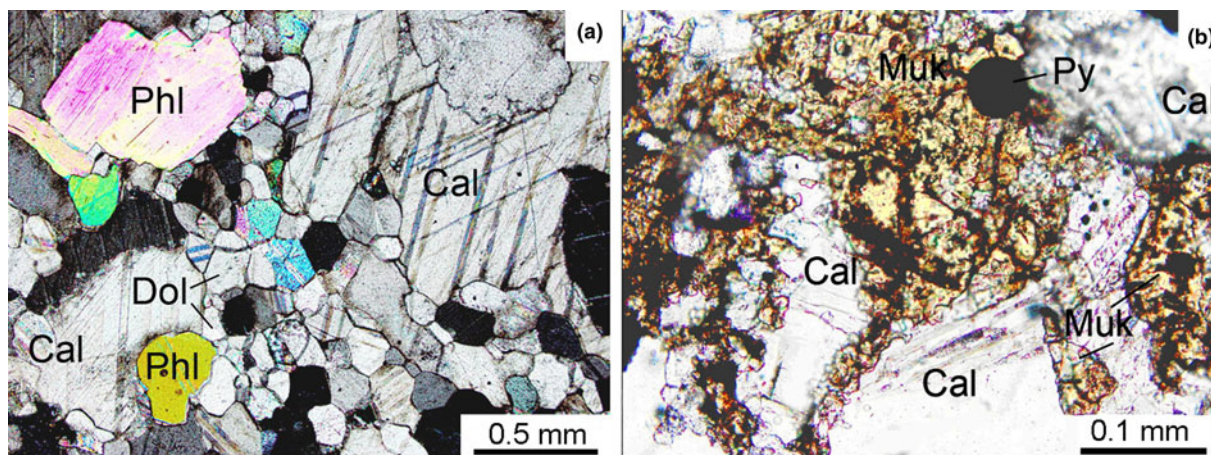
Fig. 2. Fragments of the mukhinite-bearing carbonate rock from the Svetlinsky deposit: (a) intergrowths of calcite (Cal), dolomite (Dol) and phlogopite (Phl); (b) anhedral grains of REE-rich mukhinite (Muk) in association with pyrite (Py). Photos of thin sections of in polarised light.

9.06–9.81, Pr_2O_3 3.29–3.83, Nd_2O_3 7.83–8.36, SO_3 2.64–3.09, UO_2 1.27–2.38; total 73.54–73.77 wt.% which may correspond to REE-hydroxide carbonates or high-hydrous hydroxides contaminated by inclusions of silicate and other phases.

Materials and methods

Samples and their chemical composition

The samples studied in this work were collected from carbonate veins exposed in the walls of the quarry of the Svetlinsky gold ore deposit, South Urals. A representative specimen of calcite–dolomite rock with REE-rich mukhinite, vaesite, sulvanite and patrónite is stored in the Natural Science Museum of the Ilmeny Reserve, Miass, Russia, with the catalogue number 17502.

Separation of minerals for chemical analyses was carried out using an optical microscope. The chemical composition of rock-forming minerals in polished samples and their images produced by back-scattered electrons were obtained on a REMMA-202M scanning electron microscope with an LZ-5 Link Systems energy-dispersive with a Si–Li detector at an accelerating voltage of 20 kV and a beam diameter of 1–2 μm. Correction of data was carried out using the Magallanes and ZAF procedure. Afterwards, the composition of mukhinite and some associated minerals were refined using a Cameca SX100 microanalyser at an accelerating voltage of 15 kV and an electron probe current of 40 nA. The probe standards (natural and synthetic reference materials) were: diopside (Mg, Ca and Si), jadeite (Al and Na), rhodonite (Mn), orthoclase (K), glass doped with REE at 4 wt.% (La and Ce) and 10 wt.% (Nd, Pr and Y), V_2O_3 (V), TiO_2 (Ti), Cr_2O_3 (Cr), Fe_2O_3 (Fe), Co and Ni. The detection limits of REE (ppm) are: 230 for Y, 450 for La, 430 for Ce, 770 for Pr and 1600 for Nd. Abbreviations of minerals in photographs and tables are after Warr (2021).

Raman spectroscopy

The Raman spectrum of REE-rich mukhinite was recorded from zones of ~10 μm in size on a polished thin section in the spectral range of 100–1200 cm^{-1} using a Horiba Jobin Yvon IHR 320 LabRAM Raman spectrometer, equipped with an Olympus BX41 microscope, a TV camera and a cooled CCD detector. The 632.8 nm line of a He–Ne laser (Pmax = 20 mW) served as the excitation line; the spectral slit width was 2 cm^{-1}. The scattered light was collected in the 180° reflection mode. The spectra were obtained by adding 20 intermediate spectra with an accumulation time of 10 s and processed using the Horiba *Labspec v.5* program.

Single-crystal X-ray analysis

An anhedral grain of mukhinite was extracted carefully using a polarising microscope and its quality was tested by single-crystal X-ray diffraction. Single-crystal X-ray data for mukhinite were collected at room temperature on an Xcalibur Oxford Diffraction diffractometer with a graphite monochromatised MoKα radiation source (λ = 0.71073 Å) and a CCD detector using the ω scanning mode. The *CrysAlis* software package (Oxford Diffraction, 2009) was used to determine and refine unit-cell parameters using least-square techniques, integrate data, and to correct them for background, Lorentz and polarisation effects.

The supplementary crystallographic data is deposited at CCDC/FIZ Karlsruhe database with number CSD 1893666 [https://www.ccdc.cam.ac.uk/structures/] and as Supplementary material (see below).

Results

General appearance and chemical composition of REE-rich mukhinite

Individual grains of REE-rich mukhinite do not have distinct crystallographic outlines. Their boundaries with other minerals are sharp, sinuous and smoothly curved (Fig. 5a, d). Mukhinite grains are broken by thin cracks into small blocks that preserve a common optical orientation (Fig. 3f). The colour of the mineral is dark brown in transmitted light (in thin sections) and light brown or greenish grey in reflected light.

Chemical data for V-rich epidote-group minerals from the Svetlinsky deposit together with literature data for mukhinite from other deposits are presented in Tables 2 and 3 and in Fig. 7. The assignment of the analysts to mukhinite or clinozoisite was made based on the dominant component (V or Al) at the M3 site of the crystal structure provided that all V, Cr, Fe, Mn and Mg are concentrated at this site, in accordance with Armbruster *et al.* (2006). Most formulae based on 12.5 oxides, i.e.
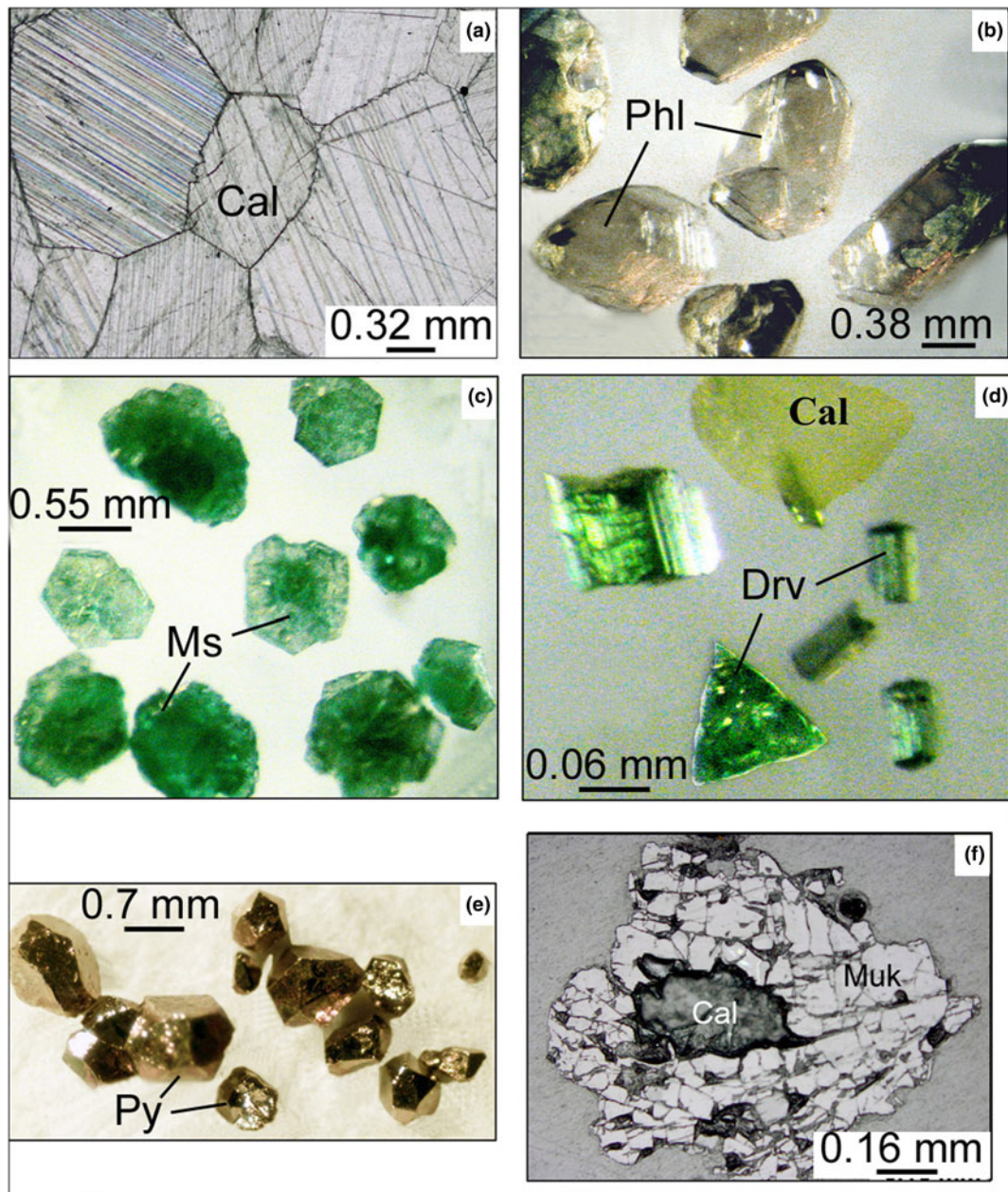
Fig. 3. Minerals associated with REE-rich mukhinite: (a) an aggregate of medium-grained calcite (Cal) – optical microscopy of a thin section); (b) fluorophlogopite (Phl) crystals; (c) bright green crystals of chromium-bearing muscovite (Ms); (d) green crystals of V- and Cr-bearing dravite (Drv) from intergrowths in calcite; (e) crystals of pyrite (Py) from intergrowths with calcite; and (f) a back-scattered electron (BSE) image of REE-rich mukhinite (Muk) in the calcite aggregate. The photos (b) to (e) are made using a stereo-microscope.

$O_{12}(OH)$, are in good agreement with the stoichiometry of epidote-group minerals.

The presence of rare-earth elements (4.0 to 9.7 wt.% of ΣREE_2O_3) in the epidote-group minerals from the Svetlinsky deposit is noteworthy. Measured rare-earth elements belong to the group of light lanthanides. Among them, La (La_2O_3 2.4–6.0 wt.%) predominates, but Ce (Ce_2O_3 0.7–1.7 wt.%) and Nd (Nd_2O_3 0.8–1.5 wt.%) are constantly present. The presence of detectable amounts of Pr (Pr_2O_3 0.1–0.4 wt.%) and Sm is very rare and was found only in some samples. Mukhinite from the Svetlinsky deposit differs significantly from REE-free mukhinite from other localities.

Raman spectroscopy

The Raman spectrum of REE-rich mukhinite is given in Fig. 8 (curve a) together with spectra of epidote and clinozoisite. The assignment of the Raman bands of epidote-group minerals is as follows (Varlamov *et al.*, 2019; Kasatkin *et al.*, 2020a; 2020b): 1000–1100 cm^{-1} is assigned to stretching vibrations of Si–O–Si fragments in the Si_2O_7 groups; and the 850 to 1000 cm^{-1} range to stretching vibrations of apical Si–O bonds. The range between 650 and 710 cm^{-1} is assigned to M–O···H bending vibrations. 300 to 610 cm^{-1} are from mixed modes and overlapping bands of M–O-stretching vibrations, as well as bending vibrations of
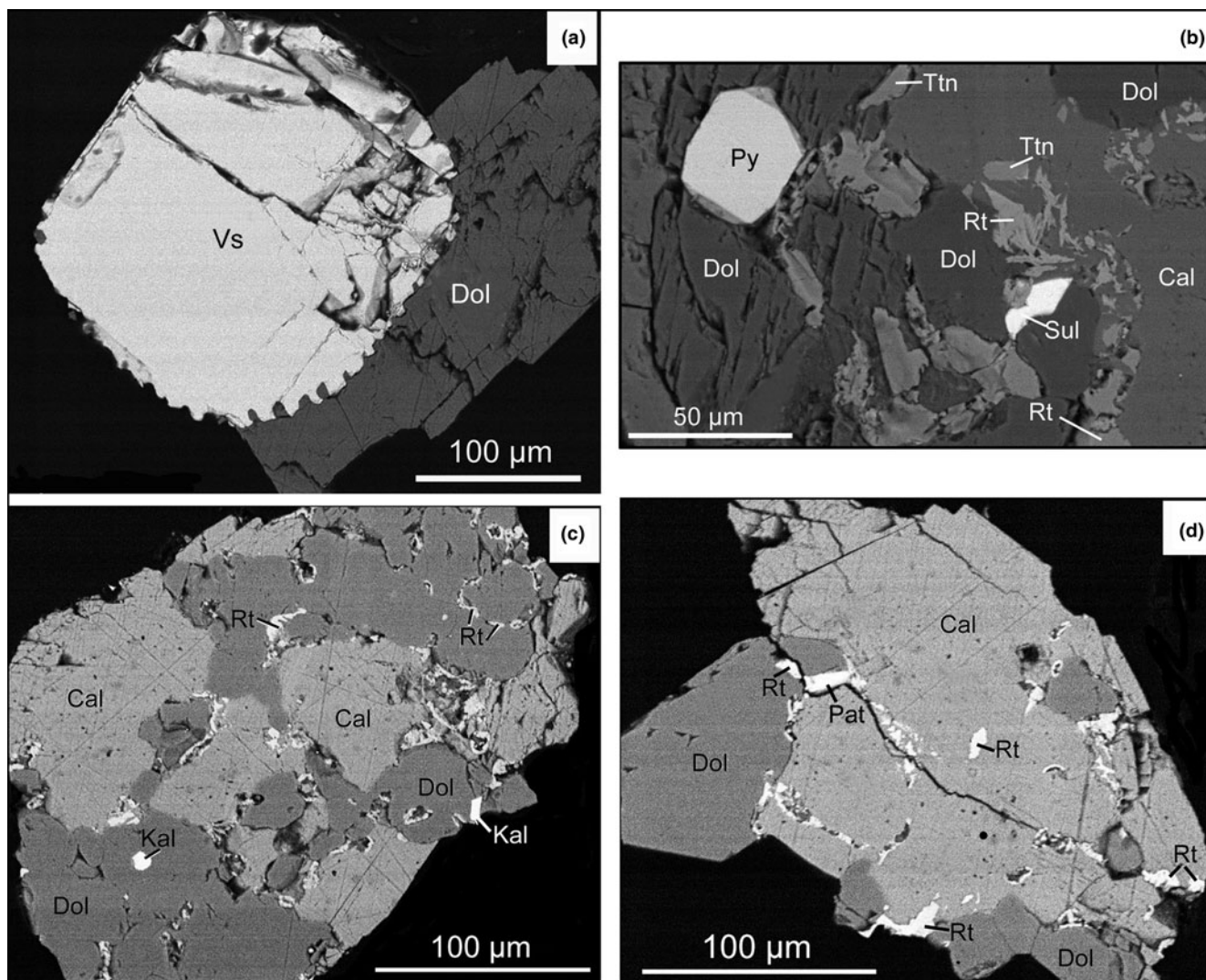
Fig. 4. BSE images of rare sulfides in phlogopite-bearing dolomite–calcite carbonatite from the Svetlinsky quarry: (a) vaesite (Vs) in association with dolomite (Dol); (b) sulvanite (Sul) in association with rutile (Rt), titanite (Ttn) and pyrite (Py); (c) kalininite (Kal) crystals; and (d) patrónite (Pat) in association with rutile (Rt) in calcite–dolomite rock.

silicate groups. Below 300 cm^{-1} bands are due to lattice modes involving REE–O-, Ca–O- and Fe^{2+}–O-stretching vibrations and librational vibrations of silicate groups.

The position of the band within the range of 1020–1200 cm^{-1} related to stretching vibrations of the Si–O–Si fragment depends on the value of the Si–O–Si angle: the higher this angle, the higher the frequency of corresponding vibrations (Chukanov, 2014). The Si–O–Si angle in the Si$_2$O$_7$ group depends on the force characteristics of a cation in the $A2$ site. In particular, the substitution of Ca with REE results in the lowering of both the Si–O–Si angle and frequency of stretching vibrations of Si–O–Si fragments (Varlamov *et al.*, 2019). As a result, the band at 1090–1094 cm^{-1} in the Raman spectra of REE-free epidote-group minerals shifts to lower frequencies in the Raman spectrum of REE-bearing mukhinite. Numerous local maxima in the range of 1000–1090 and shoulders in the range of 290–330 cm^{-1} observed in the Raman spectrum of mukhinite from the Svetlinsky deposit reflect different local situations around the Si$_2$O$_7$ group and $A2$ site, respectively.

Crystal structure of REE-rich mukhinite from the Svetlinsky deposit

The crystal structure of REE-rich mukhinite from South Urals is similar to the structures of other epidote-supergroup minerals (Armbruster *et al.*, 2006) as well as the synthetic analogue of mukhinite (Nagashima *et al.*, 2019). The epidote-type structure is based on chains of two types (Chain 1 and Chain 2) formed by edge-sharing octahedra ($M2$O$_6$ and $M1$O$_6$ octahedra, respectively). Chain 2 is decorated by additional $M3$O$_6$-octahedra, attached to the alternate sides along the chain. These chains are linked together *via* SiO$_4$-tetrahedra and Si$_2$O$_7$ disilicate groups to form a heteropolyhedral pseudo-framework (Fig. 8) with two types of cavities, occupied by large $A1$- and $A2$-cations.

A total of 3545 reflections within the sphere delimited by θ = 29.01° were measured for the sample studied. The refined monoclinic unit-cell parameters are: $a = 8.8972(11)$ Å, $b = 5.6221(6)$ Å, $c = 10.1519(12)$ Å, β = 115.169°; and $V = 459.60(11)$ Å^3. The space group $P2_1/m$ (No. 7), which is common for the epidote-supergroup

Table 1. Chemical composition of some minerals, coexisting with REE-rich mukhinite from carbonatites of the Svetlinsky deposit (wt.%).

Mineral Analysis no.	Fluoro-phlogopite 1*	Muscovite 2*	Titanite 4	Dravite 5	Andradite 6	Clinochlore 7*	Rutile 8*	Anhydrite 9*	Calcite 10*
Na_2O	nd	0.12	nd	2.00	nd	nd	nd	nd	nd
K_2O	10.12	10.46	nd	0.09	nd	nd	nd	nd	nd
CaO	nd	nd	29.90	1.07	33.32	0.30	nd	41.25	54.19
MgO	27.40	3.51	nd	10.46	0.06	34.56	nd	nd	2.06
Fe_2O_3	nd	nd	nd	nd	29.67	nd	nd	nd	nd
Al_2O_3	12.54	30.29	8.05	34.16	1.25	19.66	nd	nd	nd
V_2O_3	0.35	1.23	3.61	2.63	0.11	0.94	2.34	nd	nd
Cr_2O_3	nd	0.42	nd	0.52	0.02	nd	nd	nd	nd
SiO_2	44.86	49.42	32.05	39.58	35.76	31.12	nd	nd	nd
TiO_2	nd	0.23	26.25	nd	0.08	nd	96.55	nd	nd
Total	98.26	95.68	99.86	90.51	100.27	86.58	99.52	99.82	56.25
Formula coefficients									
Na	–	0.02	–	0.59	–	–	–		
K	0.89	0.88	–	0.02	–	–	–		
Ca	–	–	0.995	0.18	3.00	0.03	–	1.00	0.95
Mg	2.81	0.35	–	2.36	0.01	4.82	–		0.05
Fe^{+3}	–	–		–	1.87	–	–		
Al	1.02	2.36	0.30	6.25	0.12	2.17	–		
V^{+3}	0.02	0.07	0.09	0.33	0.01	0.07	0.02		
Cr	–	0.02	–	0.06	0.00	–	–		
Si	3.09	3.26	0.995	6.00	2.99	2.91			
Ti	–	0.01	0.62	–	0.00	–	0.94		
Calculation basis	22 charge units for O+F	22 charge units for O+OH	3 cations	6 Si atoms	8 cations	10 cations	1 cation	1 S atom	1 cation

'nd' – not detected.
* Analyses performed on SEM REMMA-202 M by V.A. Kotlyarov (other analyses were performed on Cameca SX100). Additionally found: Analysis 1: F 5.17 wt.%, –O≡F –2.18 wt.%, F 1.13 apfu; analysis 8: Nb_2O_5 0.63 wt.%. Nb 0.04 apfu; Analysis 9: SO_3 58.57 wt.%, S 1.00 wt.%.

minerals, was chosen on the basis of systematic absences of reflections and intensity statistics. Details of the data collection and refinement results are listed in Table 4.

The structure determination and refinement were carried out using the *JANA2006* program package (Petricek *et al.*, 2014). The initial model for the mukhinite structure refinement was based on the atomic coordinates of its synthetic analogue (Nagashima *et al.*, 2019). Atomic scattering factors and anomalous dispersion corrections from the *International Tables for Crystallography* (Prince, 2004) were used. Illustrations were produced in the *JANA2006* program package in combination with the program *DIAMOND3* (Brandenburg and Putz, 2005). Because of the complex chemical composition, the cation distribution on the structural sites was proposed, taking into account site-scattering factors, interatomic distances and ionic radii of the cations: firstly the number of electrons associated with the atoms at the site (e_{calc}) (Hawthorne *et al.*, 1995) was determined; secondly, for each value of e_{calc} the most suitable ratio between the atoms with the closest final refined amount of electrons (e_{ref}) was selected and atoms coordinates and ADPs were refined. The final refinement cycles converged to $R_1 = 3.84$ and $wR_2 = 4.97$ with GoF = 1.22 for 1160 observed reflections with $I > 2\sigma(I)$. Table 5 lists the fractional atomic coordinates, occupancy, site symmetry and equivalent isotropic atomic displacement parameters (U_{eq}). Anisotropic atomic displacement parameters (U_{ij}) are presented in Table S1 (Supplementary materials). Selected interatomic distances as well as hydrogen bonding parameters are given in Table 6.

Bond-valence sum (BVS) calculations can be used as indirect verification of mixed oxygen/hydroxyl sites in the structure. BVS calculations (Table S2) were performed using the bond-length parameters for Ca^{2+}–O, La^{3+}–O, Al^{3+}–O, V^{3+}–O, Mg^{2+}–O (Brown and Altermatt, 1985), Si^{4+}–O (Brese and O'Keeffe, 1991) and H^+–O (Brown, 2006).

The refined crystal-chemical formula of REE-rich mukhinite is $(Z = 2)$ $\{^{A1}Ca^{A2}(Ca_{0.8}REE_{0.2})\}\{^{M1}(Al_{0.95}Cr_{0.05})^{M2}Al$ $^{M3}[(V,Cr)^{3+}_{0.40}Al_{0.35}Mg_{0.25}]\}(Si_2O_7)(SiO_4)O(OH)$, which is in an excellent agreement with the empirical formula (Table 3). The smallest $M2O_6$-octahedron with the mean $M2$–O distance of 1.882 Å is occupied by Al^{3+}, while the largest $M3O_6$-octahedron (with $<M3$–O$> = 2.029$ Å) concentrates V^{3+}, Mg^{2+} and a part of Cr^{3+}. The $M1O_6$-octahedron having an intermediate size (with $<M1$–O$> = 1.915$ Å) contains a minor admixture of a cation heavier than Al^{3+}. Taking into account that the ionic radius of $^{[6]}Cr^{3+}$ (0.615 Å) is intermediate between those of $^{[6]}Al^{3+}$ and $^{[6]}V^{3+}$ (0.535 and 0.640 Å, respectively) (Shannon, 1976), we suppose that a minor admixture of Cr^{3+}, rather than V^{3+}, occurs at the $M2$ site. The incorporation of the large Mg^{2+} cation with the ionic radius of 0.72 Å (Shannon, 1976) in the $M3$ site is confirmed by the increased mean bond length in comparison with synthetic mukhinite with $M3 = V^{3+}_{0.62}Al^{3+}_{0.38}$ and $<M3$–O$> = 2.023$ Å (Nagashima *et al.*, 2019).

Members of epidote group (Armbruster *et al.*, 2006) are characterised by the predominance of divalent cations at both $A1$ and $A2$ sites of large cations. In the crystal structure of REE-rich mukhinite (Fig. 9), the $A1$ site with $<A1$–O$> = 2.585$ Å is completely occupied by Ca^{2+}, while the $A2$ site with $<A2$–O$> = 2.679$ Å hosts REE^{3+} cations (with the predominance of La^{3+}, in accordance with the chemical data) and has a mixed composition with 0.80(1) Ca apfu and 0.20(1) REE apfu, which is in a good agreement with the site scattering factor ($e_{ref} = 27.30$ epfu; $e_{calc} = 29.40$ epfu).

Thus, the structural data confirm that the mineral studied is a member of the epidote group, namely, a V-deficient, Cr-bearing and REE-rich variety of mukhinite. In particular, the data obtained confirm that V^{3+} is concentrated at the $M3$ site. The crystal structure of natural mukhinite was solved for the first time.
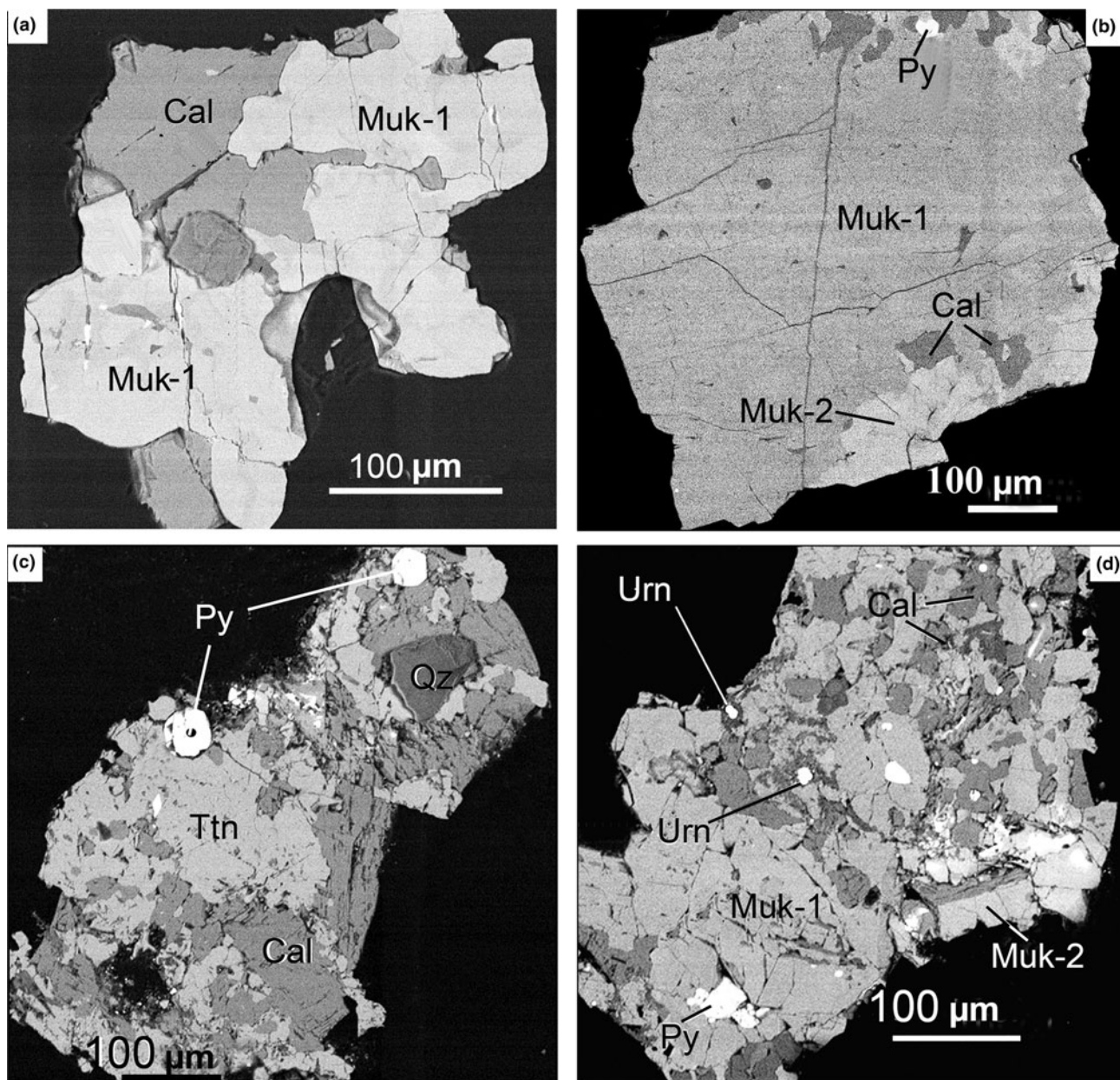
Fig. 5. REE-rich mukhinite and closely associated minerals from carbonate rocks of the Svetlinsky deposit (BSE images): (a) mukhinite individuals with sinuous induction boundaries; (b) segregation of the Muk-2 on the periphery of a Muk-1 grain; (c) aggregates of V-bearing titanite (Ttn), calcite (Cal), anhedral grain of quartz (Qz) and crystals of pyrite (Py); and (d) calcite–mukhinite aggregate with inclusions of uranium hydroxides (Urn).

Discussion

When analysing the data on the chemical composition of V- and REE-containing minerals of the epidote group from the Svetlinsky deposit and mukhinite from other localities, it turned out that there is a perfect positive correlation (with a correlation coefficient of 0.979) between the total REE content and the formula coefficient of magnesium, as well as a distinct negative correlation (with a correlation coefficient of –0.706) between the total V+Cr content and the formula coefficient of aluminium (Figs 10 and 11). Thus, the main schemes of isomorphic substitutions in these minerals are $\Sigma REE + Mg \leftrightarrow Ca + Al$ and $V+Cr \leftrightarrow Al$.

The simultaneous occurrence of significant amounts of Cr and REE in a mineral of the epidote supergroup was noted by us in the rocks of the dyke complex of the Kosyu ore field, Chetlassky Kamen, Middle Timan Mts., which belongs to the Riphean Chetlas hypabyssal complex of alkaline picrites and carbonatites (Varlamov *et al.*, 2019). This potentially new mineral is characterised by low aluminium contents. Its idealised formula is $CaCeFe^{3+}CrFe^{3+}Si_2O_7)(SiO_4)O_2$ or $CaCeFe^{3+}CrFe^{2+}(Si_2O_7)(SiO_4)O(OH)$ (depending on the valence state of iron). It is similar to mukhinite from the Svetlinsky deposit by a number of features: confinement to a carbonatite-containing complex, simultaneous occurrence of significant amounts of Cr and REE, and the presence of a magnesium impurity.

According to Armbruster *et al.* (2006), the *M*3 site is most preferable for the incorporation of Mg^{2+} and ions of transition elements (e.g. Cr, V, Mn and Fe). The authors of that paper
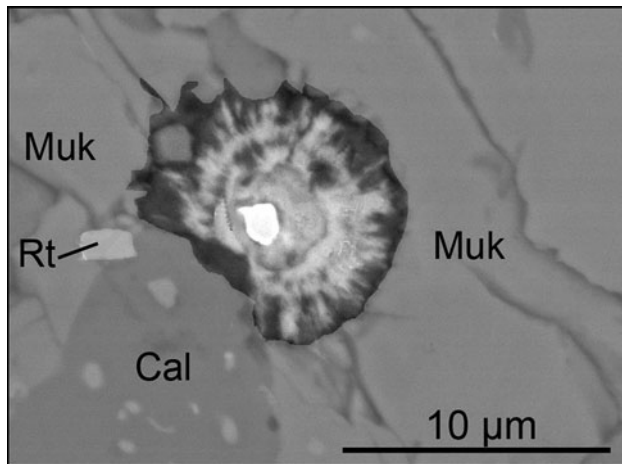
Fig. 6. BSE image of uranium (hydr)oxide (?) (white) in the core of a radiated aggregate of REE-rich minerals situated between grains of REE-rich mukhinite and calcite, in association with rutile (Rt).

recommend placing these ions in the *M*3 site when calculating empirical formulae of epidote-group minerals with $^{VI}Al \geq 2$ apfu, whereas in samples with $^{VI}Al < 2$ apfu the excess of *M*-cations other than Al should be placed in the *M*1 site. However, X-ray structural analysis shows that there is a statistical distribution of these cations over the *M* sites. For example, in the holotype sample of ferriakasakaite-(La), a part of Fe^{3+} occurs at the *M*2 site despite the *M*1 site containing 0.18 Al apfu (Nagashima *et al.*, 2015). The holotype sample of ferriallanite-(La) contains 0.06 Fe apfu at the *M*2 site despite the *M*1 site containing 0.42 Al apfu (Kolitsch *et al.*, 2012). Mukhinite from the Svetlinsky deposit is thus, one more example showing statistical distribution of a transition element over *M* sites.

On the basis of available data on chemical composition of Cr- and V-bearing epidote-group minerals from different localities one can suppose that there is a trend to the enrichment of REE-bearing samples with Cr, which may require partial substitution of trivalent cations with Mg and/or substitution of OH groups with O. Indeed, in the epidote-supergroup mineral from Middle Timan, both Ce and Cr are the species-defining components. V-bearing epidote-group minerals from the Svetlinsky deposit are characterised by lower contents of Cr and ΣREE. In mukhinite from other localities, both Cr and REE are absent or occur in trace amounts. The cause of this regularity is unclear.

The close similarity of the carbonate dykes of the Svetlinsky deposit in mineral composition and structural features indicate their simultaneous formation. The bedding of these carbonate rocks in the form of secant bodies with parallel contacts indicates their possible magmatic origin. The calcite–dolomite rock of the dyke in which REE-rich mukhinite is found, differs from the classical rare-metal carbonatites of Urals in which apatite, zircon, pyrochlore-group minerals, monazite and other rare earth minerals play a significant role among accessories (Levin *et al.*, 1978). Obviously, this is due to the difference between the primary magmas. Rare-metal carbonatites are closely related genetically to alkaline–ultrabasic magmas, and the calcite–dolomite rocks described in this paper are probably formed by magma that arose during the re-melting of marbles, limestones and serpentinite melange plates under the exposure of the heat of granite intrusions and their fluids (Kolisnichenko and Popov, 2008; Ivanov,

2011). The specific features of the chemical composition of the minerals associated with REE-rich mukhinite (Table 1), including relatively high amounts of vanadium and chromium in most accessories, fluorine in fluorophlogopite and fluoro-tremolite, as well as the appearance of uranium hydroxides reflect the specific composition of the melt that could form the carbonate dykes.

High-temperature and high-pressure conditions for the formation of the calcite–dolomite rocks have been shown by independent methods of geothermometry and geobarometry. The presence of syntactic intergrowths of various minerals (pyroxenes, amphiboles, garnets, micas and plagioclases) made it possible to determine the temperatures of crystallisation as in the range of 600–900°C (Korinevsky and Korinevsky, 2020). Such temperatures correspond to magmatic formations (carbonatites) (Shumilova *et al.*, 2012). The equilibrium pressure for these parageneses, determined using amphibole geobarometers, ranges from 8 to 12 kbar. The presence of native sulphur in carbonate rocks indicates a reducing environment for the formation of high-temperature and high-pressure carbonate melts.

According to the previous works (Kolisnichenko and Popov, 2008; Ivanov, 2011), carbonate rocks of the Svetlinsky deposit have a crustal rather than mantle origin. The carbonatite-forming magma was generated as a result of melting of marbles, limestones and serpentinite melange under the exposure of heat and fluids supplied by granite intrusions. As a result, carbonate rocks of the Svetlinsky deposit are enriched with B, V, Ni, Cr, U, REE and P and depleted in Fe and Mn. This set of elements is not typical for the classical carbonatites of the Urals (Levin *et al.*, 1978).

The composition of minerals found in veins of carbonate rocks at the Svetlinsky deposit is very similar to those from the ruby-bearing carbonatites described previously from the limestone quarry situated 14 km to the East of the Kuchinsky quarry (Kolisnichenko and Popov, 2008). A very similar association of minerals was observed in marbles from the outcrops along the Suunduk River in the South Urals (Tomilina *et al.*, 2016). There are some common features of these two localities such as the strong hydrosulfuric smell released during crushing, a bright green colour of some silicate minerals containing Cr^{3+} impurities, and the presence of noble spinel. In Gornaya Shoriya and the Urals, mukhinite was found in marbles, also in the exocontact zone of granite intrusions (Shepel and Karpenko, 1965; Tomilina *et al.*, 2016). At the Ilmeno–Vishnevogorsky complex and Svetlinsky gold deposit, low concentrations of REE, V and Cr were assumed for the original carbonate sediments (Krasnobaev *et al.*, 2013). During transformations of the sediments to a marble, the transition elements were released by hydrothermal solutions, which were activated by granite intrusions and lead to concomitant metasomatism of the rocks. In all above-listed localities, V–Cr mineralisation, including mukhinite, is considered as a late product of thermal and fluid impact of intrusive masses on the volcanogenic–sedimentary rocks, enriched initially with V, Cr, carbon and their subsequent reprocessing in regional and contact metamorphism. High contents of REE are a specific feature of V-bearing epidote-group minerals from the Svetlinsky deposit, unlike mukhinite from other deposits related to carbonatites (Shepel and Karpenko, 1965; Karpov *et al.*, 2013; Tomilina *et al.*, 2016).

Conclusions

The accessory mineralisation in carbonate rocks of the Svetlinsky gold deposit is very diverse and is individual for each dyke. Most individuals of accessory minerals have induction boundaries

Table 2. Chemical composition of REE-rich mukhinite and V^{3+},REE-rich clinozoisite from the Svetlinsky deposit, and mukhinite from other deposits in Russia (wt.%).

| | REE-rich mukhinite | | | | | | | | | V^{3+},REE-rich clinozoisite | | | | Mukhinite from other deposits in Russia | | | |
| | Muk-1 | | Muk-2 | | | | | | | | | | | | | | |
Analyses	1	2	3	4	5	6	7	8	9	10	11	12	13	14	15*	16	17
MgO	0.98	1.11	1.46	1.68	1.54	1.73	1.75	1.78	2.34	1.45	1.59	1.60	1.85	bdl	bdl	0.41	0.20
CaO	22.03	21.30	20.60	20.49	20.58	20.37	20.25	20.49	19.29	21.10	21.06	20.63	20.05	22.23	24.12	22.79	23.39
NiO	0.01	0.01	0.02	bdl	0.02	bdl	bdl	0.02	bdl	bdl	bdl	bdl	bdl	bdl	bdl	0.03	bdl
Al_2O_s	25.68	24.62	23.68	21.91	23.44	22.43	22.62	23.91	21.85	25.19	26.67	25.25	24.60	21.81	24.23	25.17	26.57
V_2O_3	5.95	5.50	7.46	6.70	7.54	6.71	6.63	6.33	5.34	5.54	4.04	4.94	4.66	11.29	7.66	9.21	7.72
Cr_2O_3	1.07	2.95	0.64	3.10	0.73	1.90	1.89	0.70	2.54	0.78	0.67	0.86	0.96	0.28	bdl	0.52	0.52
Fe_2O_3	bdl	bdl	bdl	bdl	0.09	bdl	bdl	0.02	2.34	bdl	0.02	bdl	bdl	1.31	3.48	0.01	0.02
La_2O_3	2.40	2.38	3.78	4.19	4.01	4.54	4.71	4.58	6.05	3.75	3.79	3.95	4.76	nd	nd	nd	nd
Ce_2O_3	0.70	0.76	1.18	1.21	1.36	1.25	1.30	1.27	1.74	1.11	1.27	1.30	1.38	nd	nd	nd	nd
Pr_2O_3	0.09	0.14	0.31	0.13	0.27	0.32	0.26	0.26	0.39	0.16	0.31	0.38	0.43	nd	nd	nd	nd
Nd_2O_3	0.82	0.97	1.19	1.07	1.30	1.00	1.07	1.31	1.50	1.09	1.17	1.20	1.53	nd	nd	nd	nd
ΣREE_2O_3	4.01	4.25	6.46	6.60	6.94	7.11	7.34	7.42	9.68	6.11	6.54	6.83	8.10	nd	nd	nd	nd
SiO_2	37.36	37.08	36.58	36.45	36.71	36.22	36.33	36.57	35.93	36.75	37.75	36.71	36.61	36.50	38.34	37.93	38.41
Total	97.10	96.83	96.91	96.94	97.59	96.48	96.84	97.25	99.31	96.93	98.35	96.85	96.90	93.42	98.04	96.12	96.89
Formula coefficients calculated on three Si atoms																	
Mg	0.12	0.13	0.18	0.21	0.19	0.21	0.22	0.22	0.29	0.18	0.19	0.19	0.23	0	0	0.05	0.02
Ca	1.89	1.85	1.81	1.81	1.81	1.81	1.79	1.80	1.72	1.84	1.80	1.80	1.76	1.98	2.04	1.94	1.97
Ni	0.01	0.01	0	0	0	0	0	0	0	0	0	0	0	0	0	0	0
Al	2.43	2.35	2.29	2.29	2.26	2.19	2.21	2.31	2.15	2.41	2.51	2.43	2.38	2.13	2.25	2.36	2.46
V	0.38	0.36	0.49	0.44	0.49	0.45	0.44	0.42	0.36	0.36	0.26	0.32	0.31	0.75	0.48	0.59	0.49
Cr	0.07	0.19	0.04	0.20	0.05	0.13	0.12	0.045	0.17	0.05	0.04	0.06	0.06	0.02	0	0.03	0.03
Fe	0	0	0	0	0.01	0	0	0	0.15	0	0	0	0	0.08	0	0	0
La	0.07	0.07	0.11	0.13	0.12	0.14	0.14	0.14	0.19	0.11	0.11	0.12	0.14	0	0	0	0
Ce	0.02	0.02	0.04	0.04	0.04	0.04	0.04	0.04	0.05	0.03	0.04	0.04	0.04	0	0	0	0
Pr	0	0	0.01	0	0.01	0.01	0.01	0.01	0.01	0.03	0.04	0.04	0.04	0	0	0	0
Nd	0.02	0.03	0.04	0.03	0.04	0.03	0.03	0.04	0.04	0.03	0.03	0.04	0.05	0	0	0	0
ΣREE	0.11	0.12	0.20	0.20	0.21	0.22	0.22	0.23	0.28	0.20	0.22	0.24	0.27	0	0	0	0
Si	3.00	3.00	3.00	3.00	3.00	3.00	3.00	3.00	3.00	3.00	3.00	3.00	3.00	3.00	3.00	3.00	3.00

bdl: below detection limit; nd: not detected or no data; *analysis also includes MnO 0.21 wt.%.

Notes: 1–13 are samples from carbonatites of the Svetlinsky deposit (this study): 1–2 is mukhinite with low REE contents (Muk–1), 3–9 is mukhinite with elevated REE contents (Muk–2; analysis 7 corresponds to the crystal used for the crystal structure refinement), and 10–13 is V^{3+},REE-rich clinozoisite. Other analyses: 14 – mukhinite from calcareous skarns of the Tashelginsky deposit, Gornaya Shoria (Konovalenko et al., 2012); 15 – mukhinite with moderate vanadium content from pyrite ores of the Pyrrhotite gorge deposit in Kola Peninsula (Karpov et al., 2013), 16–17 – mukhinite from marbles of the Suunduk anticlinorium near the village Kvarkeno, South Urals (Tomilina et al., 2016). In detail: 16 – from central parts of the crystals of mukhinite (average of 5 analyses), 17 – from marginal parts of the same crystals of mukhinite (average of 6 analyses). Fe is calculated as Fe_2O_3.

Table 3. Chemical composition of mukhinite from the Svetlinsky deposit (mean of 15 analyses, wt.%).

Constituent	Content	Standard deviation
MgO	1.68	0.38
CaO	20.44	0.79
La_2O_3	4.35	1.16
Ce_2O_3	1.27	0.28
Pr_2O_3	0.28	0.12
Nd_2O_3	1.21	0.22
Al_2O_3	23.76	1.52
V_2O_3	5.89	1.00
Cr_2O_3	1.48	0.86
SiO_2	36.60	0.52
H_2O	1.82*	
Total	98.78	

*Calculated from the charge-balanced empirical formula $Ca(Ca_{0.80}La_{0.13}Ce_{0.04}Nd_{0.03}Pr_{0.01})_{\Sigma1.01}(Al_{2.30}V_{0.39}Cr_{0.10}Mg_{0.21})_{\Sigma3.00}(SiO_4)(Si_2O_7)O[(OH)_{0.97}O_{0.03}]$ based on $(SiO_4)(Si_2O_7)O(OH,O)$.

indicating their joint growth with carbonates and other minerals. No signs of metasomatic replacement of any minerals by other minerals have been found. Most accessory silicates and oxides associated with mukhinite contain appreciable amounts of Cr and V.
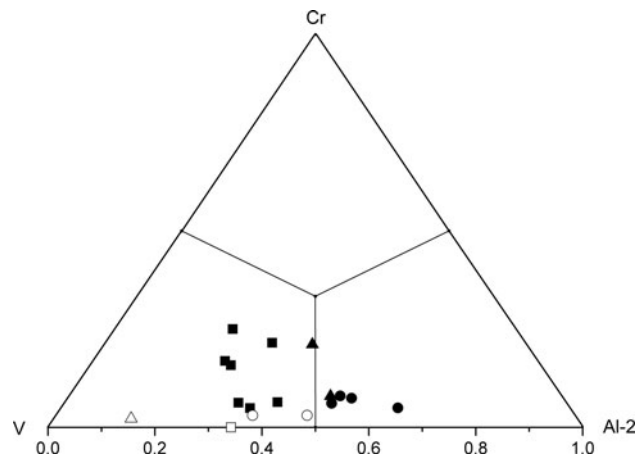

Fig. 7. Diagram showing relative contents (apfu) of the major trivalent cations at M sites in REE-rich mukhinite Muk-1, this work (black triangles); REE-rich mukhinite Muk-2, this work (black squares); V^{3+},REE-rich clinozoisite, this work (black circles); mukhinite from Kvarkeno, South Urals (open circles, Tomilina *et al.*, 2016); mukhinite from Pyrrhotite gorge, Kola Peninsula (open square, Karpov *et al.*, 2013), and mukhinite holotype sample from the Tashelginsky occurrence, Gornaya Shoria (open triangle, Konovalenko *et al.*, 2012).
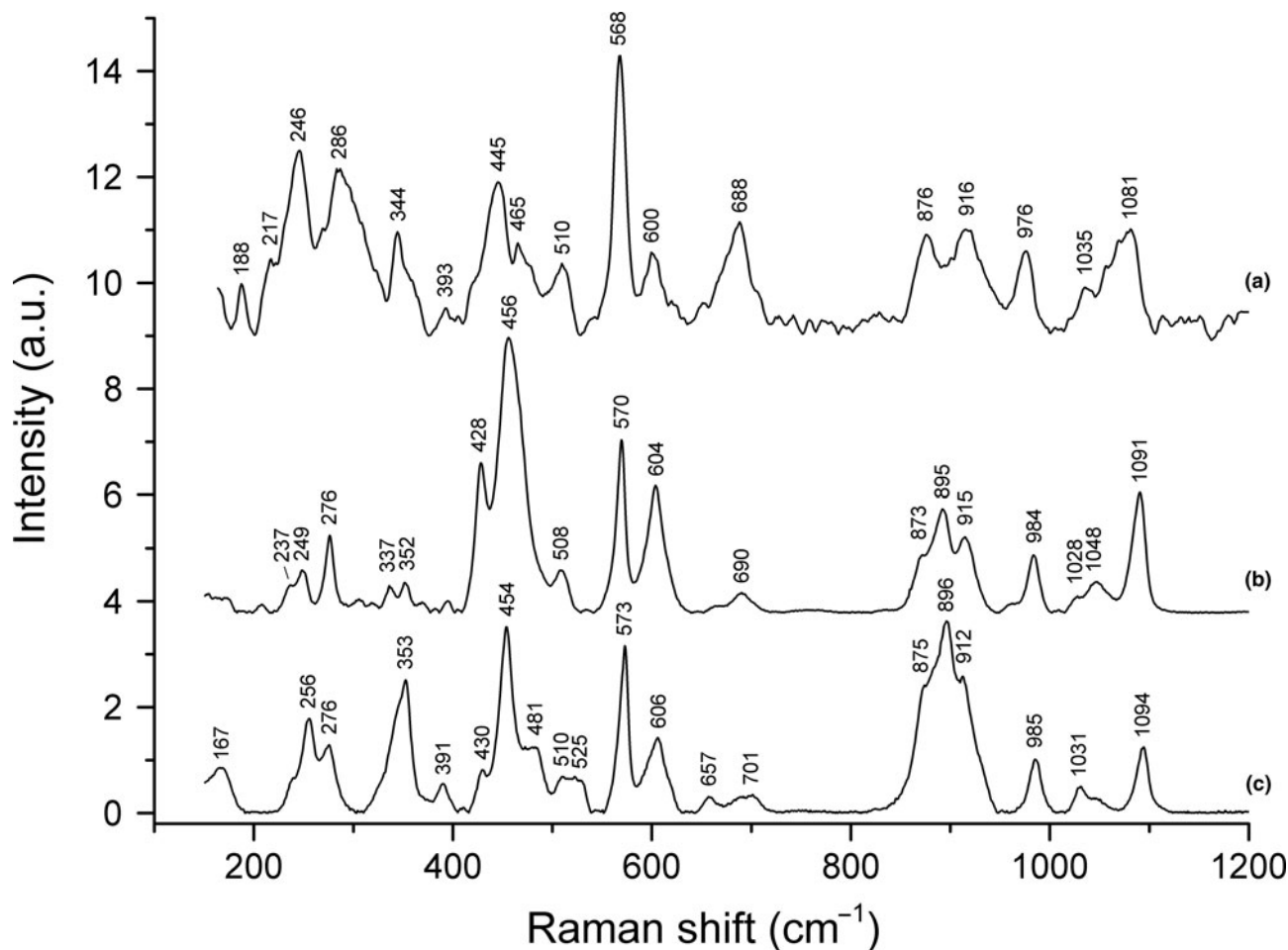

Fig. 8. (a) Raman spectra of REE-rich mukhinite from the Svetlinsky deposit. The spectra of (b) epidote and (c) clinozoisite from the RRUFF database (Lafuente *et al.*, 2015) are given for comparison.

Table 4. Crystal data, data collection and refinement procedure results for the studied crystal of mukhinite.

Crystal data

Refined formula	$(Ca_{1.75}REE_{0.25})[Al_{2.30}V_{0.39}Mg_{0.21}Cr_{0.10}]$ $(Si_2O_7)(SiO_4)O(OH)$
Formula weight (g)	488.0
Temperature (K)	293
Cell setting	Monoclinic
Space group	$P2_1/m$ (№ 11)
a (Å)	8.8972(11)
b (Å)	5.6221(6)
c (Å)	10.1519(12)
β (°)	115.169(14)
V (Å³)	459.60(11)
Z	2
Calculated density, D_x (g cm⁻³)	3.526
Crystal size (mm)	0.03 × 0.12 × 0.14
Crystal shape	Platy
Data collection	
Diffractometer	Xcalibur, Sapphire 3 (CCD-plate)
Radiation; λ (Å)	MoKα; 0.71073
Absorption coefficient, μ (mm⁻¹)	3.338
F (000)	478
Data range θ (°)	$4.01 < \theta < 29.01$
Ranges of h, k, l	$-11 < h < 12$, $-7 < k < 7$, $-13 < l < 12$
No. of measured reflections	3545
Total reflections (N_2)/observed (N_1)	1351 / 1160
Criterion for observed reflections	$I > 2\sigma(I)$
Number of refined parameters (N_{ref})	121
R_{int} (%)	3.58
Refinement	
Refinement on	Full-matrix least squares on F
Weight scheme	$1/(\sigma^2|F| + 0.0001F^2)$
R_1, wR_2 for $I > 2\sigma(I)$	3.84, 4.73
R_1, wR_2 for all data	4.65, 4.97
GoF (Goodness of fit)	1.22
Max./min. residual e^- density, (e^-Å⁻³)	0.76 / -0.65

Table 6. Selected interatomic distances in mukhinite.

A1–O7	2.309(4)		M1–O4	1.843(2)	×2
A1–O3	2.346(2)	×2	M1–O1	1.945(3)	×2
A1–O1	2.465(3)	×2	M1–O5	1.957(2)	×2
A1–O5	2.530(4)		<M1–O>	1.915	
A1–O6	2.815(3)				
A1–O9	2.995(1)	×2	M2–O3	1.856(2)	×2
<Al–O>	2.585		M2–O10	1.865(3)	×2
			M2–O6	1.924(3)	×2
A2–O7	2.293(3)		<M2–O>	1.882	
A2–O2	2.521(2)	×2			
A2–O10	2.605(3)		M3–O8	1.868(4)	
A2–O3	2.657(3)	×2	M3–O4	1.919(3)	
A2–O2	2.751(3)	×2	M3–O2	2.013(2)	×2
A2–O8	3.015(1)	×2	M3–O1	2.181(2)	×2
<A2–O>	2.679		<M3–O>	2.029	
Si1–O7	1.569(3)		Si2–O8	1.589(5)	
Si1–O9	1.635(4)		Si2–O3	1.621(2)	×2
Si1–O1	1.651(3)	×2	Si2–O9	1.628(3)	
<Si1–O>	1.627		<Si2–O>	1.615	
Si3–O2	1.626(3)	×2			
Si3–O6	1.644(4)				
Si3–O5	1.667(3)				
<Si3–O>	1.641				

the crystallisation occurred at temperatures of 560–800°C and a pressure of ~10 kbar. The carbonate rocks of the Svetlinsky deposit differ from the classical rare-metal carbonatites of the Urals in which zircon and minerals of the apatite, pyrochlore and monazite groups, as well as other rare earth minerals play a significant role among accessories.

Accessory mukhinite from the Svetlinsky gold deposit has a REE-rich, Cr-bearing and V-deficient variety. The crystal structure of natural mukhinite has been studied for the first time. The structure refinement has shown that the distribution of cations having octahedral coordination among M sites violates from the ideal scheme of the crystal-chemical formula calculation. Based on the correlation analysis of the chemical composition of mukhinite and associated V,REE-bearing clinozoisite, it was concluded that the coupled replacement of $\Sigma REE + Mg$ with $Ca + Al$

The calcite–dolomite rocks of the Svetlinsky gold deposit are probably formed by magma of crustal origin that arose during the re-melting of marbles, limestones and serpentinite melange plates under the influence of the heat of granite intrusions and their fluids. According to the data of mineral geothermobarometers,

Table 5. Fractional coordinates, site multiplicities (Mult.), equivalent displacement parameters of atoms (U_{eq}, Å²), site scattering (electrons per formula unit, epfu), mean bond distances in coordination polyhedra (Å), and site occupancies in the structure of mukhinite.

|						Site scattering (e.p.f.u.)		Bond distance (Å)		
Site	x	y	z	Mult.	$U_{eq/iso}*$	Calculated	Refined	Calculated	Refined	s.o.f.
A1	0.7610(1)	¾	0.1536(10)	2	0.0145(4)	19.48	20	2.530	2.585	Ca
A2	0.5999(1)	¾	0.4255(1)	2	0.0142(2)	27.30	27.40	2.590	2.679	$Ca_{0.8}REE_{0.2}$
M1	0	0	0	2	0.0101(5)	13.15	13.55	1.889	1.915	$Al_{0.95}Cr_{0.05}$
M2	0	0	½	2	0.0090(5)	12.86	13	1.885	1.882	Al
M3	-0.2907(1)	-¼	-0.2189(1)	2	0.0139(4)	16.96	17.19	1.973	2.029	$(V,Cr)_{0.44}Al_{0.35}Mg_{0.21}$
Si1	0.3387(2)	¾	0.0464(1)	2	0.0093(4)			1.610	1.627	Si
Si2	0.6827(2)	-¼	0.2765(1)	2	0.0098(4)			1.610	1.615	Si
Si3	0.1833(2)	¾	0.3179(1)	2	0.0087(4)			1.610	1.641	Si
O1	0.2351(3)	0.9950(4)	0.0426(2)	4	0.0130(8)					O
O2	0.3034(3)	0.9819(4)	0.3551(2)	4	0.0141(8)					O
O3	0.7929(3)	0.4869(4)	0.3430(2)	4	0.0147(8)					O
O4	-0.0522(4)	-¼	-0.1294(3)	2	0.0104(11)					O
O5	0.0412(4)	¾	0.1454(3)	2	0.0108(11)					O
O6	0.0642(4)	¾	0.4048(3)	2	0.0116(11)					O
O7	0.5146(4)	¾	0.1782(3)	2	0.0130(11)					O
O8	0.5226(5)	¼	0.3084(4)	2	0.0226(14)					O
O9	0.3674(5)	¾	-0.1028(3)	2	0.0212(13)					O
O10	0.0789(4)	¼	0.4259(3)	2	0.0112(11)					O
H^{O10}	0.052(7)	¼	0.322(3)	2	0.0141*					H
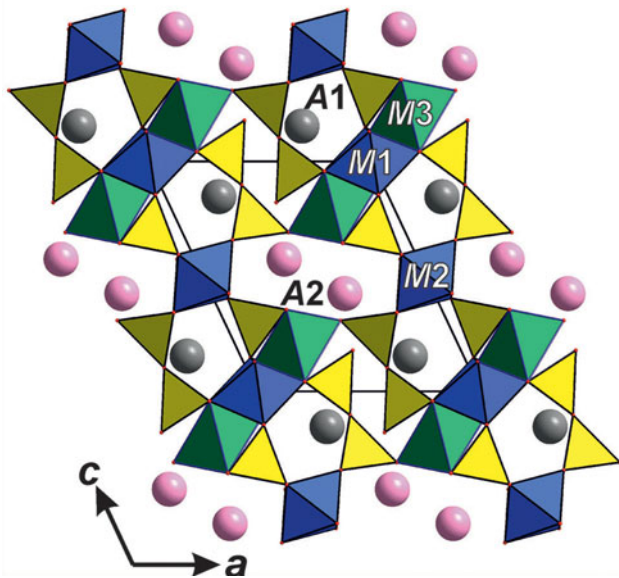
Fig. 9. The crystal structure of REE-rich mukhinite (a general view). Grey circles correspond to the *A*1 site, completely occupied by Ca, whereas pinky circles correspond to the *A*2 site, characterised by the predominance of Ca with the admixture of REE (0.20 apfu).
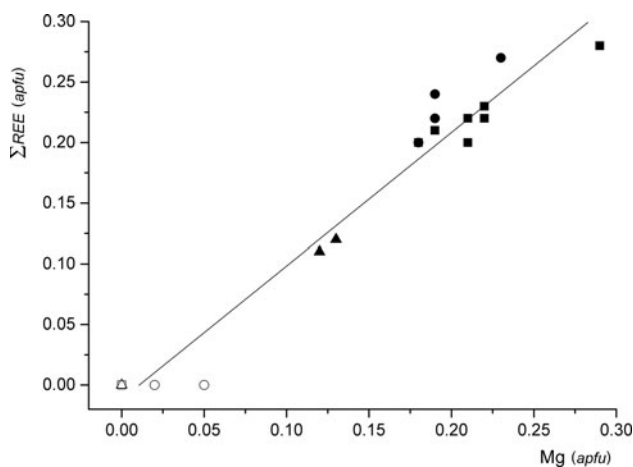

Fig. 10. Correlation between ΣREE and Mg (apfu) in V-rich epidote-group minerals. For legend, see Fig. 7.
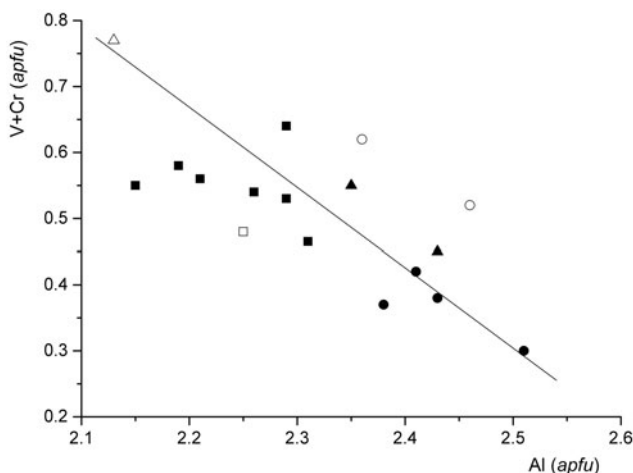

Fig. 11. Correlation between V+Cr and Al (apfu) in V-rich epidote-group minerals. For legend, see Fig. 7.

and the homovalent substitution of V+Cr for Al are the main schemes of isomorphic substitutions in these minerals.

References

Armbruster T., Bonazzi P., Akasaka M., Bermanec V., Chopin C., Gieré R., Heuss-Assbichler S., Liebscher A., Menchetti S., Pan Y. and Pasero M. (2006) Recommended nomenclature of epidote-group minerals. *European Journal of Mineralogy*, **18**, 551–567.

Bačík P. and Uher P. (2010) Dissakisite-(La), mukhinite, and clinozoisite: (V,Cr,REE)-rich members of the epidote group in amphibole-pyrite-pyrrhotite matabasic rocks from Pezinok, Rybníček mine, Western Carpathians, Slovakia. *The Canadian Mineralogist*, **48**, 523–536.

Bačík P., Uher P., Kozáková P., Števko M., Ozdín D. and Vaculovič T. (2018) Vanadian and chromian garnet- and epidote-supergroup minerals in metamorphosed Paleozoic black shales from Čierna Lehota, Strážovské vrchy Mts., Slovakia: crystal chemistry and evolution. *Mineralogical Magazine*, **82**, 889–911.

Brandenburg K. and Putz H. (2005) *DIAMOND, Version 3.* Crystal Impact GbR. Bonn, Germany.

Brese N.E. and O'Keeffe M. (1991) Bond-valence parameters for solids. *Acta Crystallographica*, B47, 192–197.

Brown I.D. (2006) *The Chemical Bond in Inorganic Chemistry: The Bond Valence Model.* Oxford University Press, Oxford, UK, 278 pp.

Brown I.D. and Altermatt D. (1985) Bond-valence parameters obtained from a systematic analysis of the Inorganic Crystal Structure Database. *Acta Crystallographica*, **B41**, 244–247.

Chukanov N.V. (2014) *Infrared Spectra of Mineral Species.* Springer Geochemistry/Mineralogy, Springer Netherlands, Dordrecht, The Netherlands.

Hawthorne F.C., Ungaretti L. and Oberti R. (1995) Site populations in minerals; terminology and presentation of results of crystal-structure refinement. *The Canadian Mineralogist*, **33**, 907–911.

Ivanov K.S. (2011) About of the nature of carbonatites of the Urals. *Lithosphere*, **1**, 20–33.

Karpov S.V., Voloshin A.V., Savchenko E.E. and Selivanova E.A. (2013) Vanadium minerals in ores of Pyrrhotite gorge (Prikhibinie, Kola peninsula). *Proceedings of the Russian Mineralogical Society*, **142**, 83–99.

Kasatkin A.V., Zubkova N.V., Pekov I.V., Chukanov N.V., Škoda R., Polekhovsky Y.S., Agakhanov A.A., Belakovskiy D.I., Kuznetsov A.M., Britvin S.N. and Pushcharovsky D.Y. (2020a) The mineralogy of the historical Mochalin Log REE deposit, South Urals, Russia. Part I. New gatelite-group minerals ferriperbøeite-(La), (CaLa$_3$)(Fe^{3+}Al$_2$Fe^{2+})[Si$_2$O$_7$][SiO$_4$]$_3$ O(OH)$_2$ and perbøeite-(La), (CaLa$_3$)(Al$_3$Fe^{2+})[Si$_2$O$_7$][SiO$_4$]. *Mineralogical Magazine*, **84**, 593–607.

Kasatkin A.V., Zubkova N.V., Pekov I.V., Chukanov N.V., Ksenofontov D.A., Agakhanov A.A., Belakovskiy D.I., Polekhovsky Y.S., Kuznetsov A.M., Britvin S.N., Pushcharovsky D.Y. and Nestola F. (2020b) The mineralogy of the historical Mochalin Log REE deposit, South Urals, Russia. Part II. Radekškodaite-(La), (CaLa$_5$)(Al$_4$Fe^{2+})[Si$_2$O$_7$][SiO$_4$]$_5$O (OH)$_3$ and radekškodaite-(Ce), (CaCe$_5$)(Al$_4$Fe^{2+})[Si$_2$O$_7$][SiO$_4$]$_5$O(OH)$_3$, two new minerals. *Mineralogical Magazine*, **84**, 839–853.

Kolisnichenko S.V. and Popov V.A. (2008) *"Russian Brazil" in the South Urals. Minerals of the valleys of Sanarka, Kamenka and Kabanka rivers. Encyclopaedia of Urals stone. Sanarka*, Chelyabinsk, Russia, 528 pp.

Kolisnichenko S.V., Popov V.A., Epanchintsev S.G. and Kuznetsov A.M. (2014) *All minerals of the South Urals. Minerals of the Chelyabinsk district. Encyclopaedia of Urals stone*. Sanarka, Chelyabinsk, Russia, 624 pp.

Kolitsch U., Mills S.J., Miyawaki R. and Blass G. (2012) Ferriallanite-(La), a new member of the epidote supergroup from the Eifel, Germany. *European Journal of Mineralogy*, **24**, 741–747.

Konovalenko S.I., Ananyev S.A. and Garmaeva S.S. (2012) Rare and new minerals of the Tashelga–Maizaskaya zone of Gornaya Shoriya, their peculiarities and nature. *Journal of Siberian Federal University. Engineering and Technologies*, **3**, 301–310.

Korinevsky V.G. and Korinevsky E.V. (2020) Isotopic evidences of magmatic nature of the dolomite-calcite bodies of the Ilmeny Mountains and the Plastovsky district of the South Urals. *Vestnik of Geosciences*, **11**, 3–19.

Korinevsky V.G., Kotlyarov V.A. and Kolisnichenko S. V. (2019) New findings of rare Ni, Zn, Cr, Cu and V sulphides in carbonatites of South Urals. *Vestnik of Institute of Geology of Komi Science Center of Ural Branch RAS*, **9**, 17–22.

Krasnobaev A.A., Pushkarev E. V., Busharina S. V. and Gottman I.A. (2013) Zirconology of clinopyroxenite of the Shigir Mountains (Ufalei Complex, Southern Urals). *Doklady Earth Sciences*, **450**, 647–651.

Lafuente B., Downs R.T., Yang H. and Stone N. (2015) The power of databases: The RRUFF project. Pp. 1–30 in: *Highlights in Mineralogical Crystallography*. De Gruyter, Germany.

Levin V.Y., Ronenson B.M. and Levina I.A. (1978) Carbonatites of the alkaline province of the Ilmeny-Vishnevogorsky Mountains in the Urals. *Doklady Akademii Nauk SSSR*, **240**, 930–933.

Nagashima M., Nishio-Hamane D., Tomita N., Minakawa T. and Inaba S. (2015) Ferriakasakaite-(La) and ferriandrosite-(La): new epidote-supergroup minerals from Ise, Mie Prefecture, Japan. *Mineralogical Magazine*, **79**, 735–753.

Nagashima M., Nishio-Hamane D., Nakano N. and Kawasaki T. (2019) Synthesis and crystal chemistry of mukhinite, V-analogue of clinozoisite on the join $Ca_2Al_3Si_3O_{12}(OH)–Ca_2Al_2VSi_3O_{12}(OH)$. *Physics and Chemistry of Minerals*, **46**, 63–76.

Oxford Diffraction (2009) *CrysAlisPro*. Oxford Diffraction Ltd, Abingdon, Oxfordshire, UK.

Petricek V., Dusek M. and Palatinus L. (2014) Crystallographic Computing System JANA2006: General features. *Zeitschrift für Kristallographie*, **229**, 345–352.

Prince E. (editor) (2004) *International Tables for Crystallography, Volume C, 3rd Edition, Mathematical, Physical and Chemical Tables*. Wiley, Chichester, UK.

Shannon R.D. (1976) Revised effective ionic radii and systematic studies of interatomic distances in halides and chalcogenides. *Acta Crystallographica*, **A32**, 751–767.

Shepel A.B. and Karpenko M.V. (1965) Mukhinite, a new vanadium species of epidote. *Doklady Akademii Nauk SSSR*, **185**, 1342–1345.

Shumilova T.G., Kovalchuk N.S., Mingalev A.N. and Divaev F.K. (2012) Isotopic composition of carbon and oxygen carbonates of carbonatites of the Kos'yu massif (Middle Timan). *Vestnik of Institute of Geology of Komi Science Center of Ural Branch RAS*, **4**, 9–13.

Tomilina A.V., Kisin A.Y., Sustavov S.G. and Rostova A.V. (2016) Mukhinite – the first find at the Urals. *Proceedings of the Russian Mineralogical Society*, **145**, 55–63.

Uher P., Kováčik M., Kubiš M., Shtukenberg A. and Ozdín D. (2008) Metamorphic vanadian-chromian silicate mineralization in carbon-rich amphibole schists from the Malé Karpaty Mountains, Western Carpathians, Slovakia. *American Mineralogist*, **93**, 63–73.

Varlamov D.A., Ermolaeva V.N., Chukanov N. V., Jančev S., Vigasina M.F. and Plechov P.Y. (2019) New Data on Epidote-Supergroup Minerals: Unusual Chemical Compositions, Typochemistry, and Raman Spectroscopy. *Geology of Ore Deposits*, **61**, 827–842.

Warr L.N. (2021) IMA–CNMNC approved mineral symbols. *Mineralogical Magazine*, **85**, 291–320, https://doi.org/10.1180/mgm.2021.43